

ON FREE FERMIONS AND PLANE PARTITIONS

O FODA, M WHEELER AND M ZUPARIC

ABSTRACT. We use free fermion methods to re-derive a result of Okounkov and Reshetikhin relating charged fermions to random plane partitions, and to extend it to relate neutral fermions to strict plane partitions.

1. INTRODUCTION

In [1], Okounkov and Reshetikhin observed that certain exponentials of bilinears in generators of a Clifford algebra generate random plane partitions, and used that observation to define and study a new class of stochastic processes. Following common usage, as for example in [2], we refer to the generators of a Clifford algebra as *free fermions*, and to exponentials of bilinears in fermions as *vertex operators*¹.

Here, we use fermion calculus² to take a closer look at the connection between vertex operators and plane partitions, and to extend this connection to another type of vertex operators and plane partitions. The free fermions that appear in [1] carry a charge³, and the corresponding plane partitions are unrestricted. The free fermions that appear in the extension discussed in this work are neutral, and the corresponding plane partitions are restricted, as we will see below.

1.1. Contents. The paper consists of two parts that are written in a way that emphasizes their similarities. The first part consists of sections **2**, **3** and **4**, which are devoted to charged fermions (two species of fermions are involved) and random plane partitions (with no restrictions). In **2**, we interpret the operators Γ_{\pm} used in [1] as specializations (by setting the variables to certain constant values) of evolution operators from an integrable hierarchy, based on charged fermions with two essential singularities in the spectral parameter [3], and study their basic properties. In **3**, we outline a proof, based on fermion calculus, that the action of Γ_{\pm} on a Young diagram μ , generates a Young diagram ν that *interlaces* with μ . In [1], the interlacing condition was obtained using properties of skew Schur functions [4]. The point of a proof based on fermion calculus is that it may be amenable to generalizations to situations where one based on symmetric functions is not readily available. In **4**, we reproduce the result of [1], that an expectation value of products of Γ_{\pm} is MacMahon's generating function of random plane partitions [4], and observe that this generating function is a specialization of a tau function (a solution of Hirota's bilinear form) of the two-dimensional Toda lattice hierarchy. We give the details for completeness, and in preparation for deriving analogous results in the following sections and in future work.

2000 *Mathematics Subject Classification.* Primary 82B20, 82B23.

Key words and phrases. Free fermions, Plane Partitions.

¹In [1], the operators that generate plane partitions are referred to as *half-vertex operators* because each can be interpreted as a specialization of one of two factors that together form a *fermion vertex operator*. Here, we interpret each as a specialization of an *evolution operator*, and simply refer to them as *vertex operators*.

²The various algebraic methods based on the Clifford algebra of free fermion operators.

³One can think of an electric charge, such as that of an electron, normalized to ± 1 .

The second part consists of sections **5**, **6** and **7**, which are devoted to neutral fermions and a restricted class of plane partitions. In **5**, we recall basic facts related to neutral fermions from an integrable hierarchy with two essential singularities in the spectral parameter, introduce analogues of the evolution operators of **2**, and study their basic properties. In **6**, we show that the neutral fermion evolution operators, with suitable specializations of the time variables, give vertex operators $\widehat{\Gamma}_{\pm}$ that act on strict Young diagrams (all parts are distinct) to generate interlacing strict Young diagrams. In **7**, we use $\widehat{\Gamma}_{\pm}$ to generate and count a class of plane partitions that satisfy two conditions: **A**. Diagonal slices are interlacing strict Young diagrams, **B**. Connected horizontal plateaux (which by condition **A** are maximally one square wide) are 2-coloured⁴. We postulate that the resulting generating function is a specialization of a tau function of the neutral fermion analogue of the two-dimensional Toda lattice hierarchy.

2. CHARGED FERMION VERTEX OPERATORS

2.1. Charged fermions. Consider two species of free fermion operators $\{\psi_m, \psi_m^*\}$, $m \in \mathbb{Z}$, with charges $\{+1, -1\}$ (independently of m) and energies m (independently of species). They generate a Clifford algebra over \mathbb{C} defined by the anti-commutation relations

$$(1) \quad \left. \begin{aligned} [\psi_m, \psi_n]_+ &= 0 \\ [\psi_m^*, \psi_n^*]_+ &= 0 \\ [\psi_m, \psi_n^*]_+ &= \delta_{m,n} \end{aligned} \right\} \forall m, n \in \mathbb{Z}$$

We are interested in computing inner products of initial and final charged fermion states, and matrix elements of operators that interpolate them. A convenient way to perform these computations starts from a representation Fock space basis vectors in terms of *Maya diagrams* [2].

2.2. Maya diagrams. A Maya diagram is an infinite one-dimensional integral lattice, or *Go board*. Each site on the lattice is labeled by its position $i \in \mathbb{Z}$. A site corresponds to an allowed energy state. The position of a site is also the corresponding energy (so in a sense, a Maya diagram is a graphical representation of the spectrum of a system).

On each site we place a *black stone* or a *white stone*. The initial vacuum state is represented by a Maya diagram with black stones at the origin ($i = 0$), and at all positive sites, and white stones at all negative sites⁵ as in Figure 1. The final vacuum state is represented by a Maya diagram with white stones at the origin ($i = 0$), and at all negative sites, and black stones at all positive sites.

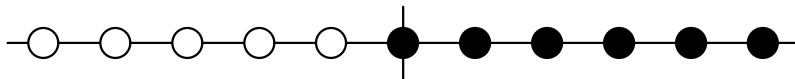


Figure 1. The Maya diagram representation of the initial ground state vector in the charged fermion Fock space. The origin is denoted by a vertical line.

⁴These results were announced in [5] and obtained independently, using different methods, in [6] and further studied in [7]. In this work, we give the details of the fermionic approach and comment on the connection to specific integrable hierarchies.

⁵This is the initial vacuum state of the sector of the Fock space with net zero charge. We will not consider vacuum states with non-zero net charges in this work, as they do not lead to different enumerative results.

A finite energy fermion basis vector corresponds to a Maya diagram such that, for a sufficiently large $N > 0$, all sites located at $i \geq N - 1$ are occupied by black stones, and sites located at $i \leq -N$ are occupied by white stones, as in Figure 2.

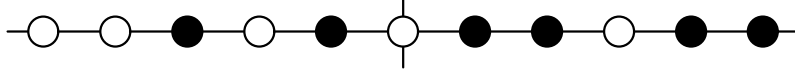


Figure 2. A Maya diagram corresponding to a finite energy charged fermion basis vector, where $N \geq 5$.

2.3. Charged fermion state vectors. We now translate the Maya diagrams to the more conventional language of state vectors. An initial state vector

$$(2) \quad |j_1, j_2, \dots\rangle, \quad j_1 < j_2 < \dots$$

corresponds to a Maya diagram with *black* stones at sites $\{j_1, j_2, \dots\}$, and white stones on all remaining sites. In other words, the corresponding Maya diagram is labeled by the positions of the *black* stones. A final state vector

$$(3) \quad \langle \dots, i_2, i_1 |, \quad \dots < i_2 < i_1$$

corresponds to a Maya diagram with *white* stones on $\{\dots, i_2, i_1\}$, and black stones on all remaining sites. In other words, the corresponding charged fermion Maya diagram is labeled by the positions of the *white* stones.

2.4. Action of charged fermions. ψ_m puts a white stone at position m (assuming a black stone is initially there). If there is already a white stone at m , it annihilates the state

$$(4) \quad \psi_m |j_1, j_2, \dots\rangle = \begin{cases} (-)^{k-1} |j_1, \dots, j_{k-1}, j_{k+1}, \dots\rangle, & m = j_k \\ 0, & \text{otherwise} \end{cases}$$

$$(5) \quad \langle \dots, i_2, i_1 | \psi_m = \begin{cases} (-)^k \langle \dots, i_{k+1}, -m, i_k, \dots, i_1 |, & i_{k+1} < -m < i_k \\ 0, & \text{otherwise} \end{cases}$$

Conversely, ψ_m^* puts a black stone at position m (assuming a white stone is initially there). If there is already a black stone at m , it annihilates the state

$$(6) \quad \psi_m^* |j_1, j_2, \dots\rangle = \begin{cases} (-)^k |j_1, \dots, j_k, m, j_{k+1}, \dots\rangle, & j_k < m < j_{k+1} \\ 0, & \text{otherwise} \end{cases}$$

$$(7) \quad \langle \dots, i_2, i_1 | \psi_m^* = \begin{cases} (-)^{k-1} \langle \dots, i_{k+1}, i_{k-1}, \dots, i_1 |, & -m = i_k \\ 0, & \text{otherwise} \end{cases}$$

The actions in (4–7) respect the anti-commutation relations in (1), and define the initial and final vacuum states, $|0\rangle$ and $\langle 0|$ by

$$(8) \quad \left. \begin{aligned} \psi_m |0\rangle &= \langle 0 | \psi_n = 0, \\ \psi_n^* |0\rangle &= \langle 0 | \psi_m^* = 0, \end{aligned} \right\} \quad \forall m < 0, n \geq 0$$

They also make it possible to create any element of the initial or final Fock spaces as a linear combination of

$$(9) \quad \left. \begin{array}{l} \psi_{m_1} \dots \psi_{m_s} \psi_{n_1}^* \dots \psi_{n_r}^* |0\rangle \\ \langle 0 | \psi_{n_r} \dots \psi_{n_1} \psi_{m_s}^* \dots \psi_{m_1}^* \end{array} \right\} \quad m_1 > \dots > m_s \geq 0, \quad n_1 < \dots < n_r < 0$$

respectively. Choosing $\langle 0|0\rangle = 1$, we obtain an inner product between the initial and final Fock spaces

$$(10) \quad \langle \dots, i_2, i_1 | j_1, j_2, \dots \rangle = \prod_{k=1}^{\infty} \delta_{i_k + j_k, 0}$$

2.5. The Lie algebra A_∞ and charged fermions. Following [3], the algebra A_∞ is the vector space

$$(11) \quad \left\{ \sum_{i,j \in \mathbb{Z}} a_{ij} : \psi_i \psi_j^* : \right\} \oplus \mathbb{C}$$

equipped with a Lie bracket⁶, where the coefficients a_{ij} satisfy the condition

$$\exists N \in \mathbb{N} \mid a_{ij} = 0, \quad \forall |i - j| > N$$

and the normal-ordered product is defined, as usual, by

$$: \psi_i \psi_j^* : := \psi_i \psi_j^* - \langle 0 | \psi_i \psi_j^* | 0 \rangle$$

2.6. A_∞ Heisenberg subalgebra. Of particular importance are the operators $H_m \in A_\infty$, where

$$(12) \quad H_m := \sum_{j \in \mathbb{Z}} : \psi_j \psi_{j+m}^* :, \quad m \in \mathbb{Z}$$

which together with the central element 1 form a Heisenberg subalgebra of A_∞

$$(13) \quad [H_m, H_n] = m \delta_{m+n, 0}, \quad \forall m, n \in \mathbb{Z}$$

Further, we also have

$$(14) \quad [H_m, \psi_n] = \psi_{-m+n}, \quad [H_m, \psi_n^*] = -\psi_{m+n}^*$$

Defining the generating functions

$$(15) \quad H_\pm(\mathbf{x}) := \sum_{m \in \pm\mathbb{N}} x_m H_m, \quad \Psi(k) := \sum_{j \in \mathbb{Z}} \psi_j k^j, \quad \Psi^*(k) := \sum_{j \in \mathbb{Z}} \psi_j^* k^j$$

and using (14), one obtains

$$(16) \quad [H_\pm(\mathbf{x}), \Psi(k)] = \sum_{m \in \pm\mathbb{N}} x_m k^m \Psi(k) := \xi_\pm(\mathbf{x}, k) \Psi(k)$$

$$(17)$$

$$(18) \quad [H_\pm(\mathbf{x}), \Psi^*(k)] = - \sum_{m \in \pm\mathbb{N}} x_m k^{-m} \Psi^*(k) := -\xi_\pm(\mathbf{x}, k^{-1}) \Psi^*(k)$$

⁶For details, please refer to [3].

2.7. Two charged fermion evolution operators. The commutators (18) imply the relations

$$(19) \quad \begin{aligned} e^{H_{\pm}(\mathbf{x})}\Psi(k)e^{-H_{\pm}(\mathbf{x})} &= \Psi(k)e^{\xi_{\pm}(\mathbf{x},k)} \\ e^{H_{\pm}(\mathbf{x})}\Psi^*(k)e^{-H_{\pm}(\mathbf{x})} &= \Psi^*(k)e^{-\xi_{\pm}(\mathbf{x},k^{-1})} \end{aligned}$$

This shows that the exponentials $e^{H_{\pm}(\mathbf{x})}$ are time evolution operators. H_+ involves the time variables $x_m, m \in \mathbb{N}$, and from ξ_+ , we see that the associated essential singularity in the spectral parameter k is at $k = \infty$. H_- involves the time variables $x_{-m}, m \in \mathbb{N}$, and from ξ_- , we see that the associated essential singularity in k is at $k = 0$. This is precisely the situation for integrable hierarchies with two essential singularities in the spectral parameter, such as the two-dimensional Toda lattice hierarchy [3, 8].

2.8. Specializing the time variables. So far, the time variables x_m are indeterminates. Setting

$$x_m = -\frac{z^{-m}}{m}, \quad \forall m \in \pm\mathbb{N}$$

where z is an indeterminate, we write $H_{\pm}(\mathbf{x}) := H_{\pm}(z)$, and $\xi_{\pm}(\mathbf{x}, k) := \xi_{\pm}(z, k)$. Then formally

$$(20) \quad \begin{aligned} \xi_+(z, k) &= -\sum_{m=1}^{\infty} \frac{1}{m} \left(\frac{k}{z}\right)^m = \log\left(1 - \frac{k}{z}\right) \\ \xi_-(z, k) &= \sum_{m=1}^{\infty} \frac{1}{m} \left(\frac{z}{k}\right)^m = -\log\left(1 - \frac{z}{k}\right) \end{aligned}$$

2.9. A_{∞} vertex operators. Given the above equation, we define the charged fermion vertex operators, $\Gamma_+(z)$ and $\Gamma_-(z)$

$$(21) \quad \Gamma_+(z) := e^{H_+(z)} = \exp\left(-\sum_{m=1}^{\infty} \frac{z^{-m}}{m} H_m\right)$$

$$(22) \quad \Gamma_-(z) := e^{-H_-(z)} = \exp\left(-\sum_{m=1}^{\infty} \frac{z^m}{m} H_{-m}\right)$$

Combining these definitions with (19) and (20), one finds

$$\begin{aligned} \Gamma_+(z)\Psi(k)\Gamma_+^{-1}(z) &= \left(1 - \frac{k}{z}\right)\Psi(k) \\ \Gamma_+(z)\Psi^*(k)\Gamma_+^{-1}(z) &= \left(\frac{kz}{kz-1}\right)\Psi^*(k) \\ \Gamma_-^{-1}(z)\Psi(k)\Gamma_-(z) &= \left(\frac{k}{k-z}\right)\Psi(k) \\ \Gamma_-^{-1}(z)\Psi^*(k)\Gamma_-(z) &= (1-kz)\Psi^*(k) \end{aligned}$$

Expanding the relations (23) in terms of operators, one obtains

$$\begin{aligned}
\sum_{j \in \mathbb{Z}} \Gamma_+(z) \psi_j \Gamma_+^{-1}(z) k^j &= \sum_{j \in \mathbb{Z}} \psi_j k^j \left(1 - \frac{k}{z}\right) \\
\sum_{j \in \mathbb{Z}} \Gamma_+(z) \psi_j^* \Gamma_+^{-1}(z) k^j &= \sum_{j \in \mathbb{Z}} \psi_j^* k^j \left(\sum_{n=0}^{\infty} \left(\frac{1}{kz}\right)^n\right) \\
\sum_{j \in \mathbb{Z}} \Gamma_-^{-1}(z) \psi_j \Gamma_-(z) k^j &= \sum_{j \in \mathbb{Z}} \psi_j k^j \left(\sum_{n=0}^{\infty} \left(\frac{z}{k}\right)^n\right) \\
\sum_{j \in \mathbb{Z}} \Gamma_-^{-1}(z) \psi_j^* \Gamma_-(z) k^j &= \sum_{j \in \mathbb{Z}} \psi_j^* k^j (1 - kz)
\end{aligned}$$

Equating powers of k in the previous expressions gives

$$\begin{aligned}
\Gamma_+(z) \psi_j \Gamma_+^{-1}(z) &= \psi_j - \frac{1}{z} \psi_{j-1} \\
\Gamma_+(z) \psi_j^* \Gamma_+^{-1}(z) &= \sum_{n=0}^{\infty} \frac{1}{z^n} \psi_{j+n}^* \\
\Gamma_-^{-1}(z) \psi_j \Gamma_-(z) &= \sum_{n=0}^{\infty} z^n \psi_{j+n} \\
\Gamma_-^{-1}(z) \psi_j^* \Gamma_-(z) &= \psi_j^* - z \psi_{j-1}^*
\end{aligned}$$

Given the definitions in (21–22) of the vertex operators, one has the commutation relation

$$\begin{aligned}
\Gamma_+(z) \Gamma_-(z') &= e^{H_+(z)} e^{-H_-(z')} \\
&= e^{[H_+(z), -H_-(z')]} e^{-H_-(z')} e^{H_+(z)} \\
&= e^{[H_+(z), -H_-(z')]} \Gamma_-(z') \Gamma_+(z)
\end{aligned}$$

Given that

$$\begin{aligned}
[H_+(z), -H_-(z')] &= \sum_{m=1}^{\infty} \sum_{n=1}^{\infty} \frac{1}{mn} z^{-m} (z')^n [H_m, H_{-n}] \\
&= \sum_{m=1}^{\infty} \sum_{n=1}^{\infty} \frac{1}{mn} z^{-m} (z')^n m \delta_{m,n} \\
&= \sum_{m=1}^{\infty} \frac{1}{m} \left(\frac{z'}{z}\right)^m = -\log \left(1 - \frac{z'}{z}\right)
\end{aligned}$$

we find

$$(23) \quad \Gamma_+(z) \Gamma_-(z') = \left(1 - \frac{z'}{z}\right)^{-1} \Gamma_-(z') \Gamma_+(z)$$

which is the basic commutation relation of charged fermion vertex operators.

3. YOUNG DIAGRAMS

Consider the Young diagram of a partition of an integer into integral parts as in Figure 3. The boxes have coordinates (i, j) , $i, j \geq 1$.

Definition 1. A hook h of a Young diagram is the set of boxes

$$h(p, q|j) = \left\{ \bigcup_{k=0}^p (j+k, j) \right\} \cup \left\{ \bigcup_{l=0}^{q-1} (j, j+l) \right\}, \quad p \geq 0, q \geq 1$$

and a full Young diagram μ is the union of hooks

$$(24) \quad \mu = \bigcup_{j=1}^r h(p_j, q_j|j)$$

for some $r \geq 1$, and $p_1 > \dots > p_r \geq 0$, $q_1 > \dots > q_r \geq 1$.

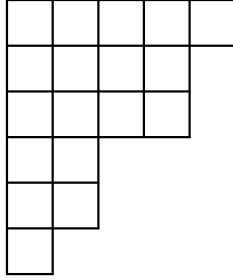


Figure 3. A Young diagram corresponding to the partition of $18 = 5+4+4+2+2+1$.

3.1. Interlacing Young diagrams.

Definition 2. Given the partition $\mu = \{\mu_1, \dots, \mu_l\}$, with $\mu_1 \geq \dots \geq \mu_l > \mu_{l+1} \equiv 0$, we say that the partition ν interlaces μ , and write $\nu \prec \mu$, when $\mu_j \geq \nu_j \geq \mu_{j+1}$, $\forall 1 \leq j \leq l$.

An example of interlacing Young diagrams is in Figure 4.

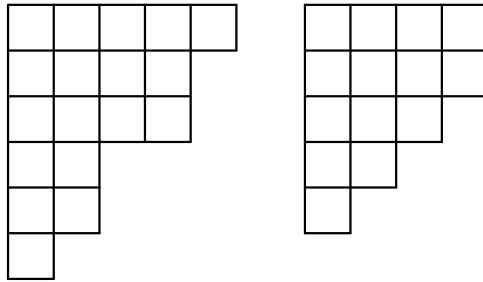


Figure 4. Interlacing Young diagrams.

Let μ be the partition given by (24), and consider the set of diagrams

$$\mathcal{D}_\mu := \left\{ \bigcup_{j=1}^r h(p'_j, q'_j|j) \mid p_j \geq p'_j \geq p_j - 1, q_j \geq q'_j \geq q_{j+1} + 1, \forall 1 \leq j \leq r \right\}$$

where $q_{r+1} \equiv 0$ and $h(-1, q'_r | r) \equiv \emptyset$. Furthermore, let $\mathcal{Y}_\mu \subseteq \mathcal{D}_\mu$ be the subset of all diagrams in \mathcal{D}_μ which are Young diagrams. Then \mathcal{Y}_μ is exactly the set of all Young diagrams that interlace μ . In other words

$$\mathcal{Y}_\mu = \{\nu \mid \nu \prec \mu\}$$

3.2. Generating interlacing Young diagrams. Every Maya diagram in (the charge-0 sector of) the initial Fock space may be represented uniquely in the form

$$|\mu\rangle := (-)^\kappa \psi_{m_1} \dots \psi_{m_r} \psi_{n_1}^* \dots \psi_{n_r}^* |0\rangle = (-)^\kappa \overleftarrow{\prod}_{j=1}^r \psi_{m_j} \overleftarrow{\prod}_{k=1}^r \psi_{n_k}^* |0\rangle$$

and every Maya diagram in (the charge-0 sector of) the final Fock space may be represented uniquely in the form

$$\langle\mu| := (-)^\kappa \langle 0 | \psi_{n_r} \dots \psi_{n_1} \psi_{m_r}^* \dots \psi_{m_1}^* = (-)^\kappa \langle 0 | \overrightarrow{\prod}_{j=1}^r \psi_{n_j} \overrightarrow{\prod}_{k=1}^r \psi_{m_k}^*$$

$m_1 > \dots > m_r \geq 0$, $n_1 < \dots < n_r < 0$, with $\kappa := \sum_{k=1}^r (m_k + k)$. The arrows on the products on the right hand sides indicate that the fermion operators in the product are ordered as shown explicitly on the left hand sides (which makes a difference as these are anti-commuting operators).

Therefore, every (charge-0) Maya diagram in the initial (respectively, final) Fock space is uniquely associated with a set of integers $m_1 > \dots > m_r \geq 0$, $n_1 < \dots < n_r < 0$, and by choosing the integers in (24) to be

$$p_j = m_j, \quad q_j = -n_j, \quad \forall 1 \leq j \leq r$$

we obtain a bijection between any (charge-0) Maya diagram in the initial (respectively, final) Fock space and the corresponding partition.

Lemma 1. *Let $|\mu\rangle$ and $\langle\mu|$ be the initial and final state vectors corresponding to the partition μ . Then*

$$(25) \quad \langle\nu|\Gamma_+(z)|\mu\rangle = \begin{cases} z^{|\nu|-|\mu|}, & \nu \prec \mu \\ 0, & \text{otherwise} \end{cases}$$

$$(26) \quad \langle\mu|\Gamma_-(z)|\nu\rangle = \begin{cases} z^{|\mu|-|\nu|}, & \nu \prec \mu \\ 0, & \text{otherwise} \end{cases}$$

Proof.

$$\begin{aligned} \Gamma_+(z)|\mu\rangle &= (-)^\kappa \Gamma_+(z) \overleftarrow{\prod}_{j=1}^r \psi_{m_j} \overleftarrow{\prod}_{k=1}^r \psi_{n_k}^* |0\rangle \\ &= (-)^\kappa \overleftarrow{\prod}_{j=1}^r \left(\Gamma_+(z) \psi_{m_j} \Gamma_+^{-1}(z) \right) \overleftarrow{\prod}_{k=1}^r \left(\Gamma_+(z) \psi_{n_k}^* \Gamma_+^{-1}(z) \right) |0\rangle \\ (27) \quad &= (-)^\kappa \overleftarrow{\prod}_{j=1}^r \left(\psi_{m_j} - \frac{1}{z} \psi_{(m_j-1)} \right) \overleftarrow{\prod}_{k=1}^r \left(\sum_{i=0}^{\infty} \frac{1}{z^i} \psi_{(n_k+i)}^* \right) |0\rangle \end{aligned}$$

Consider the action of the second product from the left in the above equation, which we call P on the vacuum $|0\rangle$.

$$\begin{aligned} P|0\rangle &= \prod_{k=1}^r \left(\sum_{i=0}^{\infty} \frac{1}{z^i} \psi_{(n_k+i)}^* \right) |0\rangle \\ &= \left(\sum_{i=0}^{\infty} \frac{1}{z^i} \psi_{(n_1+i)}^* \right) \left(\sum_{i=0}^{\infty} \frac{1}{z^i} \psi_{(n_2+i)}^* \right) \cdots \left(\sum_{i=0}^{\infty} \frac{1}{z^i} \psi_{(n_r+i)}^* \right) |0\rangle \end{aligned}$$

Split the first sum from the left into two parts to obtain

$$\begin{aligned} P|0\rangle &= \left(\sum_{i=0}^{-n_1+n_2-1} \frac{1}{z^i} \psi_{(n_1+i)}^* + \frac{1}{z^{n_2-n_1}} \sum_{i=0}^{\infty} \frac{1}{z^i} \psi_{(n_2+i)}^* \right) \\ &\quad \times \left(\sum_{i=0}^{\infty} \frac{1}{z^i} \psi_{(n_2+i)}^* \right) \cdots \left(\sum_{i=0}^{\infty} \frac{1}{z^i} \psi_{(n_r+i)}^* \right) |0\rangle \end{aligned}$$

Using the identity

$$\left(\sum_{i=0}^{\infty} \frac{1}{z^i} \psi_{(n+i)}^* \right) \left(\sum_{i=0}^{\infty} \frac{1}{z^i} \psi_{(n+i)}^* \right) = 0$$

which follows directly by expanding the sums and using the anti-commutation relation (1), we obtain

$$P|0\rangle = \left(\sum_{i=0}^{-n_1+n_2-1} \frac{1}{z^i} \psi_{(n_1+i)}^* \right) \left(\sum_{i=0}^{\infty} \frac{1}{z^i} \psi_{(n_2+i)}^* \right) \cdots \left(\sum_{i=0}^{\infty} \frac{1}{z^i} \psi_{(n_r+i)}^* \right) |0\rangle$$

This procedure can then be performed on the second sum from the left, and so on, until one reaches the last sum, which truncates using the fact that ψ_n^* annihilates the vacuum $|0\rangle$ for all $n \geq 0$. Hence

$$P|0\rangle = \left(\sum_{i=0}^{-n_1+n_2-1} \frac{1}{z^i} \psi_{(n_1+i)}^* \right) \left(\sum_{i=0}^{-n_2+n_3-1} \frac{1}{z^i} \psi_{(n_2+i)}^* \right) \cdots \left(\sum_{i=0}^{-n_r-1} \frac{1}{z^i} \psi_{(n_r+i)}^* \right) |0\rangle$$

Using the above result in (27), we obtain

$$(28) \quad \Gamma_+(z)|\mu\rangle = (-)^{\kappa} \prod_{j=1}^r \left(\psi_{m_j} - \frac{1}{z} \psi_{(m_j-1)} \right) \prod_{k=1}^r \left(\sum_{i=0}^{-n_k+n_{(k+1)}-1} \frac{1}{z^i} \psi_{(n_k+i)}^* \right) |0\rangle$$

where we have defined $n_{r+1} = 0$. Analogously to the proof of (28), we have

$$\begin{aligned} \langle \mu | \Gamma_-(z) &= (-)^{\kappa} \langle 0 | \prod_{j=1}^r \psi_{n_j} \prod_{k=1}^r \psi_{m_k}^* \Gamma_-(z) \\ &= (-)^{\kappa} \langle 0 | \prod_{j=1}^r \left(\Gamma_-^{-1}(z) \psi_{n_j} \Gamma_-(z) \right) \prod_{k=1}^r \left(\Gamma_-^{-1}(z) \psi_{m_k}^* \Gamma_-(z) \right) \\ &= (-)^{\kappa} \langle 0 | \prod_{j=1}^r \left(\sum_{i=0}^{\infty} z^i \psi_{(n_j+i)} \right) \prod_{k=1}^r \left(\psi_{m_k}^* - z \psi_{(m_k-1)}^* \right) \\ (29) \quad &= (-)^{\kappa} \langle 0 | \prod_{j=1}^r \left(\sum_{i=0}^{-n_j+n_{j+1}-1} z^i \psi_{(n_j+i)} \right) \prod_{k=1}^r \left(\psi_{m_k}^* - z \psi_{(m_k-1)}^* \right) \end{aligned}$$

It is readily seen that exactly all of the Young diagrams present in \mathcal{Y}_μ are reproduced in the expansions of (28) and (29), but with weighting factors of z . Letting

$$m_j \geq m'_j \geq m_j - 1, \quad -n_j \geq -n'_j \geq -n_{j+1} + 1, \quad \forall 1 \leq j \leq r$$

$$n_{r+1} \equiv 0, \quad h(-1, -n'_r | r) \equiv \emptyset$$

(27) is a sum of all weighted Young diagrams of the form

$$\prod_{j=1}^r z^{m'_j - m_j} z^{-n'_j + n_j} \bigcup_{k=1}^r h(m'_k, -n'_k | k)$$

whilst (29) is a sum of all weighted Young diagrams of the form

$$\prod_{j=1}^r z^{m_j - m'_j} z^{-n_j + n'_j} \bigcup_{k=1}^r h(m'_k, -n'_k | k)$$

In other words

$$\begin{aligned} \Gamma_+(z) |\mu\rangle &= \sum_{\nu \prec \mu} z^{|\nu| - |\mu|} |\nu\rangle \\ \langle \mu | \Gamma_-(z) &= \sum_{\nu \prec \mu} z^{|\mu| - |\nu|} \langle \nu | \quad \square \end{aligned}$$

The above results are known, but in [1] they were obtained using the relationship of charged vertex operators and skew Schur functions and the properties of the latter. The above proofs rely only on fermion calculus.

4. PLANE PARTITIONS

In this section, following [1], we use the above result, namely that charged fermion vertex operators act on Young diagrams to produce new Young diagrams that interlace with the first, to count plane partitions. An example of a plane partition is in Figure 5. The basic observation here, also due to [1], is that adjacent diagonal slices of plane partitions are interlacing Young diagrams. The diagonal slices of the plane partition in Figure 5 are shown on a planar representation of the same plane partition in Figure 6.

Definition 3. A plane partition π is a collection of integers $\pi(i, j) \geq 0$ assigned to each of the coordinate-labelled boxes (i, j) , restricted by the conditions $\pi(i + 1, j) \leq \pi(i, j)$, $\pi(i, j + 1) \leq \pi(i, j)$, $\forall i, j \geq 1$, and the finiteness condition $\lim_{i \rightarrow \infty} \pi(i, j) = \lim_{j \rightarrow \infty} \pi(i, j) = 0$.

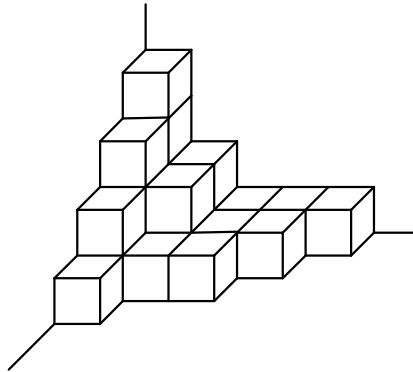


Figure 5. A plane partition.

4.1. Diagonal slices. The interlacing condition on Young diagrams can be used to construct plane partitions. Given a plane partition π , decompose it into its diagonal slices, which are the Young diagrams μ_m , $m \in \mathbb{Z}$:

$$\mu_m = \begin{cases} \{\pi(-m+1, 1), \pi(-m+2, 2), \dots\}, & m \leq 0 \\ \{\pi(1, m+1), \pi(2, m+2), \dots\}, & m \geq 0 \end{cases}$$

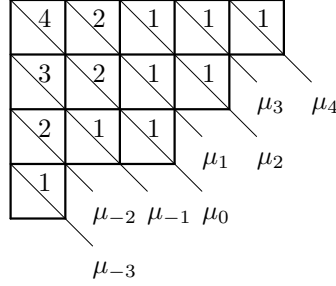


Figure 6. A planar representation of the plane partition in Figure 5 and its diagonal slices. The integers in the boxes are the heights of the corresponding columns.

Then successive diagonal slices of π are interlacing Young diagrams, in the sense that

$$(30) \quad \emptyset = \mu_{-M} \prec \dots \prec \mu_{-1} \prec \mu_0 \succ \mu_1 \succ \dots \succ \mu_N = \emptyset$$

for sufficiently large $M, N \in \mathbb{N}$. Since we understand interlacing Young diagrams in the context of fermion calculus, we can use (30) to construct plane partitions in the same formalism. Consider, for instance, the scalar product

$$(31) \quad S_A(q) := \langle 0 | \prod_{j=1}^{\infty} \Gamma_+ \left(q^{\frac{-2j+1}{2}} \right) \prod_{k=1}^{\infty} \Gamma_- \left(q^{\frac{2k-1}{2}} \right) | 0 \rangle$$

$$(32) \quad = \sum_{\mu} \langle 0 | \prod_{j=1}^{\infty} \Gamma_+ \left(q^{\frac{-2j+1}{2}} \right) | \mu \rangle \langle \mu | \prod_{k=1}^{\infty} \Gamma_- \left(q^{\frac{2k-1}{2}} \right) | 0 \rangle$$

where q is an indeterminate and \sum_{μ} denotes a sum over all Young diagrams μ . We know that $\Gamma_+(z)|\mu\rangle$ and $\langle\mu|\Gamma_-(z)$ generate all Young diagrams ν that are interlacing with μ , with weightings given by (25–26). It follows that (32) generates a weighting equal to

$$\prod_{j=1}^M \langle \nu_{-j} | \Gamma_+ \left(q^{\frac{-2j+1}{2}} \right) | \nu_{-j+1} \rangle \prod_{k=1}^N \langle \nu_{k-1} | \Gamma_- \left(q^{\frac{2k-1}{2}} \right) | \nu_k \rangle = \prod_{j=-M}^N q^{|\nu_j|}$$

for all sequences of Young diagrams of the form

$$\emptyset = \nu_{-M} \prec \dots \prec \nu_{-1} \prec \nu_0 \succ \nu_1 \dots \succ \nu_N = \emptyset$$

which, as we know, are in one-to-one correspondence with plane partitions. Hence

$$S_A(q) = \sum_{\pi} q^{|\pi|}$$

where \sum_{π} denotes a sum over all plane partitions π , and $|\pi|$ is the weight of the plane partition (the number of boxes). Applying the commutation relation (23) successively to (31), one recovers MacMahon's product form of the generating function $S_A(q)$:

$$(33) \quad S_A(q) = \prod_{n=1}^{\infty} \left(\frac{1}{1-q^n} \right)^n$$

This is the result of [1]. This ends our review of known results in the context of integrable hierarchies based on charged fermions, and their derivation in the language of fermion calculus.

4.2. The charged fermion two-dimensional Toda lattice hierarchy. Let $\mathbf{z} = \{z_1, z_2, \dots\}$ be an infinite set of variables, and $s_Y(\mathbf{z})$ be the Schur function associated to the Young diagram Y [4]. The generating function in (33) is the specialization of

$$(34) \quad S_A = \sum_Y s_Y(x_1, x_2, \dots) s_Y(y_1, y_2, \dots) = \prod_{i,j=1}^{\infty} \frac{1}{1-x_i y_j}$$

obtained by setting $\{\mathbf{x}\} = \{\mathbf{y}\} = \{q^{\frac{1}{2}}, q^{\frac{3}{2}}, \dots\}$. Under the change of variables

$$x'_n = \sum_{j=1}^{\infty} \frac{x_j^n}{n}, \quad y'_n = \sum_{j=1}^{\infty} \frac{y_j^n}{n}$$

one can rewrite (34) as

$$(35) \quad S_A = \sum_Y \chi_Y(x'_1, x'_2, \dots) \chi_Y(y'_1, y'_2, \dots)$$

where χ_Y is the character polynomial associated to Y [4]. S_A is related to the two-dimensional Toda hierarchy as follows. From [10], the general solution of the initial value problem of the two-dimensional Toda lattice is a tau function of the form

$$(36) \quad \tau(s, \mathbf{x}', \mathbf{y}') = \sum_{Y_1, Y_2 \subset (s-m) \times (n-s)} A(s, Y_1, Y_2) \chi_{Y_1}(x'_1, x'_2, \dots) \chi_{Y_2}(y'_1, y'_2, \dots)$$

where $s \in \mathbb{Z}$ labels the lattice sites, Y_1 and Y_2 are Young diagrams restricted to a rectangle of size $(s-m) \times (n-s)$, and $A(s, Y_1, Y_2)$ are scalar coefficients that encode the initial value data as defined explicitly in [10]. It is straightforward to start from (36), set $A(s, Y_1, Y_2) = \delta_{Y_1, Y_2}$, take the limits $m \rightarrow -\infty$ and $n \rightarrow \infty$, while satisfying the two-dimensional Toda bilinear identity, and show that (36) is a tau function ⁷.

⁷This connection to the two-dimensional Toda lattice hierarchy is subtle because taking the large lattice limit is non-trivial [10].

5. NEUTRAL FERMION VERTEX OPERATORS

5.1. **Neutral fermions.** In this section, we recall analogues of the properties discussed in **2**, but now for neutral fermions. Following [3], we define the neutral fermion operators $\{\phi_m\}$ in terms of $\{\psi_m, \psi_m^*\}$

$$(37) \quad \phi_m := \frac{1}{\sqrt{2}} \left(\psi_m + (-)^m \psi_{-m}^* \right), \quad m \in \mathbb{Z}$$

which are linear combinations of the charged fermions that remain invariant under the isomorphisms that define the generators of the algebra B_∞ as a subalgebra of A_∞ . More precisely, B_∞ is generated by all $X \in A_\infty$ such that $\sigma_0(X) = X$, where $\sigma_0(\psi_m) := (-)^m \psi_{-m}^*$ and $\sigma_0(\psi_m^*) := (-)^m \psi_{-m}$.

Given (37), it is easy to show that the neutral fermions satisfy the anti-commutation relation

$$(38) \quad [\phi_m, \phi_n]_+ = (-)^m \delta_{m+n,0}$$

5.2. **Half-line Maya diagrams.** Considering the neutral fermions in their own right, one can show that only one half of a Maya diagram is modified under the action of ϕ_m . In other words, for neutral fermions, we can use the usual Maya diagrams of **2**, but with the following restrictions.

All initial states are such that there are *white stones* at all negative sites. In the initial vacuum state there are black stones at the origin and all positive sites, as in Figure 7.

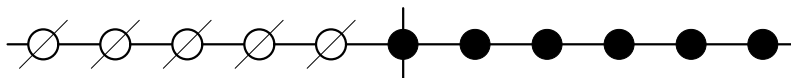


Figure 7. The Maya diagram representation of the ground state vector in the neutral fermion Fock space. The site at the origin is denoted with a vertical line. All sites to the left of the origin are frozen to be white. This is indicated with the diagonal lines.

Finite energy initial states contain a finite number of white stones at the origin and/or finite distance positive sites. An example is in Figure 8.

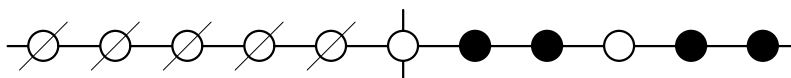


Figure 8. A Maya diagram corresponding to a finite energy neutral fermion basis vector. All sites to the left of the origin are frozen to be white.

Accordingly, all final states are such that there are *black stones* at all positive sites. In the final vacuum state there are white stones at the origin and all negative sites. Finite energy final states contain a finite number of black stones at the origin and/or finite distance negative sites. We will refer to the Maya diagrams that are relevant to neutral fermion states as *half-line Maya diagrams*.

5.3. **Neutral fermion state vectors.** Given the above definition, the state vectors (2) – (3) in **2** remain as before, but now we have

$$0 \leq j_1 < j_2 < \dots, \quad \dots < i_2 < i_1 \leq 0$$

5.4. Action of neutral fermions. For $m > 0$, ϕ_m puts a white stone at position m (assuming a black stone is initially there), otherwise it annihilates the state

$$(39) \quad \phi_{(m>0)}|j_1, j_2, \dots\rangle = \begin{cases} (-)^{m+k-1}|j_1, \dots, j_{k-1}, j_{k+1}, \dots\rangle, & m = j_k \\ 0, & \text{otherwise} \end{cases}$$

and

$$(40) \quad \langle \dots, i_2, i_1 | \phi_{(m>0)} = \begin{cases} (-)^{m+k} \langle \dots, i_{k+1}, -m, i_k, \dots, i_1 |, & i_{k+1} < -m < i_k \\ 0, & \text{otherwise} \end{cases}$$

For $m < 0$, ϕ_m puts a black stone at position $-m$ (assuming a white stone is initially there), otherwise it annihilates the state

$$(41) \quad \phi_{(m<0)}|j_1, j_2, \dots\rangle = \begin{cases} (-)^k |j_1, \dots, j_k, -m, j_{k+1}, \dots\rangle, & j_k < -m < j_{k+1} \\ 0, & \text{otherwise} \end{cases}$$

and

$$(42) \quad \langle \dots, i_2, i_1 | \phi_{(m<0)} = \begin{cases} (-)^{k-1} \langle \dots, i_{k+1}, i_{k-1}, \dots, i_1 |, & m = i_k \\ 0, & \text{otherwise} \end{cases}$$

For $m = 0$, ϕ_0 acts on the site at the origin as follows

$$(43) \quad \phi_0|j_1, j_2, \dots\rangle = \begin{cases} \frac{1}{\sqrt{2}}|0, j_1, j_2, \dots\rangle, & j_1 \neq 0 \\ \frac{1}{\sqrt{2}}|j_2, \dots\rangle, & j_1 = 0 \end{cases}$$

and

$$(44) \quad \langle \dots, i_2, i_1 | \phi_0 = \begin{cases} \frac{1}{\sqrt{2}} \langle \dots, i_2, i_1, 0 |, & i_1 \neq 0 \\ \frac{1}{\sqrt{2}} \langle \dots, i_2 |, & i_1 = 0 \end{cases}$$

5.5. The Lie algebra B_∞ and neutral fermions. Following [3], the Lie algebra B'_∞ , which is isomorphic to B_∞ , is generated by the bilinears

$$(45) \quad \left\{ \sum_{i, j \in \mathbb{Z}} b_{ij} : \phi_i \phi_j : \right\}$$

where the coefficients b_{ij} are constrained by the condition

$$\exists N \in \mathbb{N} \mid b_{ij} = 0, \quad \forall |i + j| > N$$

5.6. B_∞ Heisenberg subalgebra. Similarly to **2**, we are interested in the Heisenberg subalgebra generated by $\lambda_m \in B'_\infty$, where

$$(46) \quad \lambda_m := \frac{1}{2} \sum_{j \in \mathbb{Z}} (-)^{j+1} \phi_j \phi_{-j-m}, \quad m \in \mathbb{Z}_{\text{odd}}$$

satisfy the commutation relations

$$(47) \quad [\lambda_m, \lambda_n] = \frac{m}{2} \delta_{m+n, 0}, \quad \forall m, n \in \mathbb{Z}_{\text{odd}}$$

5.7. **Two neutral fermion evolution operators.** We begin by defining

$$\begin{aligned}\Lambda_{\pm}(\mathbf{x}_{\text{odd}}) &:= \sum_{m \in \pm \mathbb{N}_{\text{odd}}} x_m \lambda_m \\ \Phi(k) &:= \sum_{j \in \mathbb{Z}} \phi_j k^j\end{aligned}$$

Using $[\lambda_m, \phi_n] = \phi_{n-m}$, $\forall m \in \mathbb{Z}_{\text{odd}}, n \in \mathbb{Z}$, it follows that

$$[\Lambda_{\pm}(\mathbf{x}_{\text{odd}}), \Phi(k)] = \sum_{m \in \pm \mathbb{N}_{\text{odd}}} x_m k^m \Phi(k) := \zeta_{\pm}(\mathbf{x}_{\text{odd}}, k) \Phi(k)$$

The last commutator implies

$$(48) \quad e^{\Lambda_{\pm}(\mathbf{x}_{\text{odd}})} \Phi(k) e^{-\Lambda_{\pm}(\mathbf{x}_{\text{odd}})} = \Phi(k) e^{\zeta_{\pm}(\mathbf{x}_{\text{odd}}, k)}$$

5.8. **Specializing the time variables.** Setting

$$x_m = \frac{2}{m} z^{-m}, \quad \forall m \in \mathbb{Z}_{\text{odd}}$$

and writing $\Lambda_{\pm}(\mathbf{x}_{\text{odd}}) := \Lambda_{\pm}(z)$, $\zeta_{\pm}(\mathbf{x}_{\text{odd}}, k) := \zeta_{\pm}(z, k)$ under this specialization, we formally have

$$(49) \quad \begin{aligned}\zeta_{+}(z, k) &= \sum_{m \in \mathbb{N}_{\text{odd}}} \frac{2}{m} \left(\frac{k}{z} \right)^m = \log \left(\frac{z+k}{z-k} \right) \\ \zeta_{-}(z, k) &= - \sum_{m \in \mathbb{N}_{\text{odd}}} \frac{2}{m} \left(\frac{z}{k} \right)^m = \log \left(\frac{k-z}{k+z} \right)\end{aligned}$$

5.9. **Neutral fermion vertex operators.** $\widehat{\Gamma}^{+}(z)$ is defined as

$$(50) \quad \widehat{\Gamma}_{+}(z) := e^{\Lambda_{+}(z)} = \exp \left(\sum_{m \in \mathbb{N}_{\text{odd}}} \frac{2}{m} z^{-m} \lambda_m \right)$$

and $\widehat{\Gamma}_{-}(z)$ is defined as

$$(51) \quad \widehat{\Gamma}_{-}(z) := e^{-\Lambda_{-}(z)} = \exp \left(\sum_{m \in \mathbb{N}_{\text{odd}}} \frac{2}{m} z^m \lambda_{-m} \right)$$

Combining these definitions with the equations (48) and (49), we have

$$\widehat{\Gamma}_{+}(z) \Phi(k) \widehat{\Gamma}_{+}(-z) = \Phi(k) \left(\frac{z+k}{z-k} \right)$$

$$\widehat{\Gamma}_{-}(-z) \Phi(k) \widehat{\Gamma}_{-}(z) = \Phi(k) \left(\frac{k-z}{k+z} \right)$$

These relations contain information about the time evolution of a neutral fermion (for specialized values of the time variables), which is revealed by writing the generating function $\Phi(k)$ in its sum form, and expanding formally:

$$\sum_{j \in \mathbb{Z}} \widehat{\Gamma}_+(z) \phi_j \widehat{\Gamma}_+(-z) k^j = \sum_{j \in \mathbb{Z}} \phi_j k^j \left(1 + 2 \sum_{n=1}^{\infty} \left(\frac{k}{z} \right)^n \right)$$

$$\sum_{j \in \mathbb{Z}} \widehat{\Gamma}_-(-z) \phi_j \widehat{\Gamma}_-(z) k^j = \sum_{j \in \mathbb{Z}} \phi_j k^j \left(1 + 2 \sum_{n=1}^{\infty} (-)^n \left(\frac{z}{k} \right)^n \right)$$

Equating powers of k in the previous expressions gives

$$(52) \quad \widehat{\Gamma}_+(z) \phi_j \widehat{\Gamma}_+(-z) = \phi_j + 2 \sum_{n=1}^{\infty} \frac{1}{z^n} \phi_{j-n}$$

$$(53) \quad \widehat{\Gamma}_-(-z) \phi_j \widehat{\Gamma}_-(z) = \phi_j + 2 \sum_{n=1}^{\infty} (-z)^n \phi_{j+n}$$

Given the definitions (50) – (51) of the vertex operators

$$\begin{aligned} \widehat{\Gamma}_+(z) \widehat{\Gamma}_-(z') &= e^{\Lambda_+(z)} e^{-\Lambda_-(z')} \\ &= e^{[\Lambda_+(z), -\Lambda_-(z')]} e^{-\Lambda_-(z')} e^{\Lambda_+(z)} \\ &= e^{[\Lambda_+(z), -\Lambda_-(z')]} \widehat{\Gamma}_-(z') \widehat{\Gamma}_+(z) \end{aligned}$$

and given that

$$\begin{aligned} [\Lambda_+(z), -\Lambda_-(z')] &= \sum_{m \in \mathbb{N}_{\text{odd}}} \sum_{n \in \mathbb{N}_{\text{odd}}} \frac{4}{mn} z^{-m} (z')^n [\lambda_m, \lambda_{-n}] \\ &= \sum_{m \in \mathbb{N}_{\text{odd}}} \sum_{n \in \mathbb{N}_{\text{odd}}} \frac{4}{mn} z^{-m} (z')^n \frac{m}{2} \delta_{m,n} \\ &= \sum_{m \in \mathbb{N}_{\text{odd}}} \frac{2}{m} \left(\frac{z'}{z} \right)^m = \log \left(\frac{z+z'}{z-z'} \right) \end{aligned}$$

we find

$$(54) \quad \widehat{\Gamma}_+(z) \widehat{\Gamma}_-(z') = \left(\frac{z+z'}{z-z'} \right) \widehat{\Gamma}_-(z') \widehat{\Gamma}_+(z)$$

which is the basic commutation relation of neutral fermion vertex operators.

6. STRICT YOUNG DIAGRAMS

Recalling the restriction on half-line Maya diagrams discussed in **5**, any half-line Maya diagram in the sector of initial states with the vacuum vector in Figure **7** (which is the only sector that we are interested in), may be represented uniquely by

$$(55) \quad |\widehat{\mu}\rangle := \alpha(-)^r \phi_{m_1} \dots \phi_{m_{2r}} |0\rangle = \alpha(-)^r \prod_{j=1}^{2r} \phi_{m_j} |0\rangle$$

whilst any half-line Maya diagram in the space of final states may be represented uniquely by

$$(56) \quad \langle \widehat{\mu} | := \alpha(-)^{r+|\widehat{\mu}|} \langle 0 | \phi_{-m_{2r}} \dots \phi_{-m_1} = \alpha(-)^{r+|\widehat{\mu}|} \langle 0 | \prod_{j=1}^{2r} \phi_{-m_j}$$

where $m_1 > \dots > m_{2r} \geq 0$, $|\widehat{\mu}| = \sum_{j=1}^{2r} m_j$, and

$$(57) \quad \alpha := \begin{cases} 1, & m_{2r} \geq 1 \\ \sqrt{2}, & m_{2r} = 0 \end{cases}$$

The strict Young diagram $\widehat{\mu} = \{m_1, \dots, m_{2r}\}$ corresponds to the initial state (55), and to the final state (56), where the circumflex indicates that the Young diagram is strict: No two (non-zero length) parts have equal length.

6.1. Interlacing strict Young diagrams. One defines interlacing strict Young diagrams precisely as in the case of random (non-strict) Young diagrams.

6.2. Generating interlacing strict Young diagrams.

Lemma 2. *Let $|\widehat{\mu}\rangle$ and $|\widehat{\nu}\rangle$ be the initial state and final state representation, (55)-(56) respectively, of the strict partition $\widehat{\mu} = \{m_1, \dots, m_{2r}\}$. Then*

$$(58) \quad \langle \widehat{\nu} | \widehat{\Gamma}_+(z) | \widehat{\mu} \rangle = \begin{cases} 2^{n(\widehat{\nu}|\widehat{\mu})} z^{|\widehat{\nu}|-|\widehat{\mu}|}, & \widehat{\nu} \prec \widehat{\mu} \text{ and } n(\widehat{\nu}) = n(\widehat{\mu}) \\ (-)^{n(\widehat{\mu})} 2^{n(\widehat{\nu}|\widehat{\mu}) + \frac{1}{2}z^{|\widehat{\nu}|-|\widehat{\mu}|}}, & \widehat{\nu} \prec \widehat{\mu} \text{ and } n(\widehat{\nu}) = n(\widehat{\mu}) - 1 \\ 0, & \text{otherwise} \end{cases}$$

$$(59) \quad \langle \widehat{\mu} | \widehat{\Gamma}_-(z) | \widehat{\nu} \rangle = \begin{cases} 2^{n(\widehat{\nu}|\widehat{\mu})} z^{|\widehat{\mu}|-|\widehat{\nu}|}, & \widehat{\nu} \prec \widehat{\mu} \text{ and } n(\widehat{\nu}) = n(\widehat{\mu}) \\ (-)^{n(\widehat{\mu})} 2^{n(\widehat{\nu}|\widehat{\mu}) + \frac{1}{2}z^{|\widehat{\mu}|-|\widehat{\nu}|}}, & \widehat{\nu} \prec \widehat{\mu} \text{ and } n(\widehat{\nu}) = n(\widehat{\mu}) - 1 \\ 0, & \text{otherwise} \end{cases}$$

where $n(\widehat{\mu})$ denotes the number of non-zero elements in $\widehat{\mu}$, $n(\widehat{\nu}|\widehat{\mu})$ denotes the number of non-zero elements in $\widehat{\nu}$, not present in $\widehat{\mu}$.

Proof. Set $m_{2r+1} \equiv -1$. Then we have

$$(60) \quad \begin{aligned} \widehat{\Gamma}_+(z) | \widehat{\mu} \rangle &= \alpha(-)^r \widehat{\Gamma}_+(z) \prod_{j=1}^{2r} \phi_{m_j} | 0 \rangle \\ &= \alpha(-)^r \prod_{j=1}^{2r} \left(\widehat{\Gamma}_+(z) \phi_{m_j} \widehat{\Gamma}_+(-z) \right) | 0 \rangle \\ &= \alpha(-)^r \prod_{j=1}^{2r} \left(\phi_{m_j} + 2 \sum_{i=1}^{\infty} \frac{1}{z^i} \phi_{(m_j-i)} \right) | 0 \rangle \end{aligned}$$

Consider the action of the product in the above equation, which we call \widehat{P} , on the vacuum $|0\rangle$.

$$\begin{aligned} \widehat{P}|0\rangle &= \left(\phi_{m_1} + 2 \sum_{i=1}^{\infty} \frac{1}{z^i} \phi_{(m_1-i)} \right) \\ &\times \left(\phi_{m_2} + 2 \sum_{i=1}^{\infty} \frac{1}{z^i} \phi_{(m_2-i)} \right) \dots \left(\phi_{m_{2r}} + 2 \sum_{i=1}^{\infty} \frac{1}{z^i} \phi_{(m_{2r}-i)} \right) | 0 \rangle \end{aligned}$$

Split the first sum from the left into parts and rewrite it as

$$\begin{aligned} \widehat{P}|0\rangle &= \left(\phi_{m_1} + 2 \sum_{i=1}^{m_1-m_2-1} \frac{1}{z^i} \phi_{(m_1-i)} + \frac{1}{z^{m_1-m_2}} \phi_{m_2} \right. \\ &\quad \left. + \frac{1}{z^{m_1-m_2}} (\phi_{m_2} + 2 \sum_{i=1}^{\infty} \frac{1}{z^i} \phi_{(m_2-i)}) \right) \prod_{j=2}^{2r} \left(\phi_{m_j} + 2 \sum_{i=1}^{\infty} \frac{1}{z^i} \phi_{(m_j-i)} \right) |0\rangle \end{aligned}$$

Using the identity

$$\left(\phi_m + 2 \sum_{i=1}^{\infty} \frac{1}{z^i} \phi_{(m-i)} \right) \left(\phi_m + 2 \sum_{i=1}^{\infty} \frac{1}{z^i} \phi_{(m-i)} \right) = 0$$

which follows by expanding each sum (including all terms up to ϕ_{-m} as all of these will contribute to the required result on the left hand side) and using the anti-commutation relation (38), we obtain

$$\begin{aligned} \widehat{P}|0\rangle &= \left(\phi_{m_1} + 2 \sum_{i=1}^{m_1-m_2-1} \frac{1}{z^i} \phi_{(m_1-i)} + \frac{1}{z^{m_1-m_2}} \phi_{m_2} \right) \\ &\quad \times \left(\phi_{m_2} + 2 \sum_{i=1}^{\infty} \frac{1}{z^i} \phi_{(m_2-i)} \right) \cdots \left(\phi_{m_{2r}} + 2 \sum_{i=1}^{\infty} \frac{1}{z^i} \phi_{(m_{2r-i})} \right) |0\rangle \end{aligned}$$

This procedure can then be performed on the second sum from the left, and so on, until one reaches the last sum, which truncates because ϕ_m annihilates $|0\rangle$ for all $m < 0$. Hence

$$\widehat{P}|0\rangle = \prod_{j=1}^{2r} \left(\phi_{m_j} + 2 \sum_{i=1}^{m_j-m_{j+1}-1} \frac{1}{z^i} \phi_{(m_j-i)} + \frac{1}{z^{m_j-m_{j+1}}} \phi_{m_{j+1}} \right) |0\rangle$$

Using the above result in (60), we obtain

$$\begin{aligned} \widehat{\Gamma}_+(z)|\widehat{\mu}\rangle &= \alpha(-)^r \prod_{j=1}^{2r} \left(\phi_{m_j} + 2 \sum_{i=1}^{m_j-m_{j+1}-1} \frac{1}{z^i} \phi_{(m_j-i)} + \frac{1}{z^{m_j-m_{j+1}}} \phi_{m_{j+1}} \right) |0\rangle \\ (61) \quad &= \sum_{\substack{\widehat{\nu} \prec \widehat{\mu} \\ n(\widehat{\nu})=n(\widehat{\mu})}} 2^{n(\widehat{\nu}|\widehat{\mu})} z^{|\widehat{\nu}|-|\widehat{\mu}|} |\widehat{\nu}\rangle + (-)^{n(\widehat{\mu})} \sqrt{2} \sum_{\substack{\widehat{\nu} \prec \widehat{\mu} \\ n(\widehat{\nu})=n(\widehat{\mu})-1}} 2^{n(\widehat{\nu}|\widehat{\mu})} z^{|\widehat{\nu}|-|\widehat{\mu}|} |\widehat{\nu}\rangle \end{aligned}$$

It is instructive to figure out the origin of the factors of 2 in (61). Recall that $\widehat{\mu}$ is a strict partition with parts of lengths $m_1 > \cdots > m_{2r} \geq 0$, and that the action of $\widehat{\Gamma}_+(z)$ reduces the heights of the parts of $\widehat{\mu}$ or leaves them invariant. Consider the right hand side of first line of (61). The j -th factor in the product describes the evolution of the j -th part of $\widehat{\mu}$, which has length m_j . From the forms of the terms in this factor, we see that there are 3 possibilities:

The first term leads to a part of length m_j , so there is no change in length, and no new factors are introduced. The second term leads to a part of length $m_j - i$, $1 \leq i \leq (m_j - m_{j+1} - 1)$ which does not occur in $\widehat{\mu}$, a factor of z^{-i} is introduced (that keeps track of the change in length) as well as a factor of 2. The third term leads to a part of length m_{j+1} , which is different from the original length of m_j but is a length that occurs in $\widehat{\mu}$, a factor of $z^{-m_j+m_{j+1}}$ is introduced, but no factor of 2.

What we learn from this is that, while powers of z keep track of changes in lengths, every time that a totally new length appears, we acquire an extra factor of 2. This explains the factors of 2 in the second line of (61).

Further, notice that the result of (61) has two terms. The first is a sum over all partitions $\widehat{\nu}$ that have the same number of non-zero parts as $\widehat{\mu}$. The second is a sum over all partitions $\widehat{\nu}$ with one non-zero part less than $\widehat{\mu}$.

The factor of $(-)^{n(\widehat{\mu})}\sqrt{2}$ in the second term accounts for the relative minus sign and valuation of α , as defined in (57), between the two types of partitions.

Analogously to the proof of (61), we have

$$\begin{aligned}
 \langle \widehat{\mu} | \widehat{\Gamma}_-(z) &= \alpha(-)^{r+|\widehat{\mu}|} \langle 0 | \prod_{j=1}^{2r} \phi_{-m_j} \widehat{\Gamma}_-(z) = \alpha(-)^{r+|\widehat{\mu}|} \langle 0 | \prod_{j=1}^{2r} \left(\widehat{\Gamma}_-(-z) \phi_{-m_j} \widehat{\Gamma}_-(z) \right) \\
 &= \alpha(-)^{r+|\widehat{\mu}|} \langle 0 | \prod_{j=1}^{2r} \left(\phi_{-m_j} + 2 \sum_{i=1}^{\infty} (-z)^i \phi_{(-m_j+i)} \right) \\
 &= \alpha(-)^{r+|\widehat{\mu}|} \langle 0 | \prod_{j=1}^{2r} \left(\phi_{-m_j} + 2 \sum_{i=1}^{m_j-m_{j+1}-1} (-z)^i \phi_{(-m_j+i)} + (-z)^{m_j-m_{j+1}} \phi_{-m_{j+1}} \right) \\
 &= \sum_{\substack{\widehat{\nu} \prec \widehat{\mu} \\ n(\widehat{\nu})=n(\widehat{\mu})}} 2^{n(\widehat{\nu}|\widehat{\mu})} z^{|\widehat{\mu}|-|\widehat{\nu}|} \langle \widehat{\nu} | + (-)^{n(\widehat{\mu})} \sqrt{2} \sum_{\substack{\widehat{\nu} \prec \widehat{\mu} \\ n(\widehat{\nu})=n(\widehat{\mu})-1}} 2^{n(\widehat{\nu}|\widehat{\mu})} z^{|\widehat{\mu}|-|\widehat{\nu}|} \langle \widehat{\nu} | \quad \square
 \end{aligned}$$

The proof is completed by taking appropriate inner products.

7. DIAGONALLY STRICT PLANE PARTITIONS

Definition 4. A *diagonally strict plane partition* $\widehat{\pi}$ is a plane partition whose diagonal slices, given by

$$\widehat{\mu}_m = \begin{cases} \{\widehat{\pi}(-m+1, 1), \widehat{\pi}(-m+2, 2), \dots\}, & m \leq 0 \\ \{\widehat{\pi}(1, m+1), \widehat{\pi}(2, m+2), \dots\}, & m \geq 0 \end{cases}$$

are all strict Young diagrams.

An example of a diagonally strict plane partition is in Figure 9. The diagonals are shown on a planar representation in Figure 10.

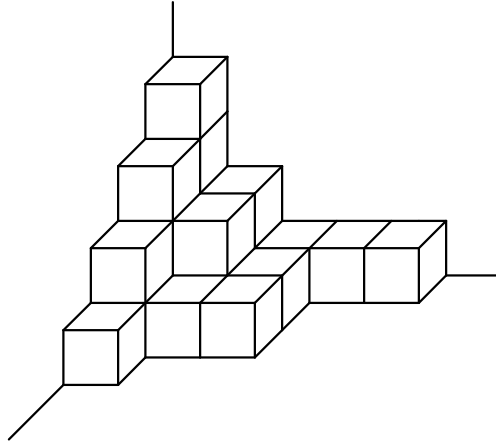


Figure 9. A diagonally strict plane partition. Notice that all connected horizontal plateaux are at most 1 square wide: there is at most one way to move from one square to another square at the same level, without changing levels.

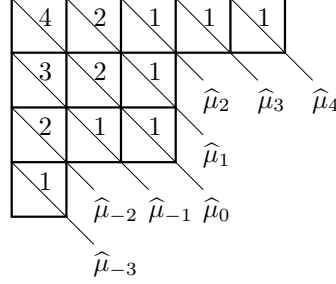


Figure 10. A planar representation of the diagonally strict plane partition in Figure 9 and its diagonal slices. The integers in the boxes are the heights of the corresponding columns.

7.1. Strict diagonal slices.

Definition 5. Given a diagonally strict plane partition $\hat{\pi}$, consider only those points (i, j) for which $\hat{\pi}(i, j) \neq 0$. We say that a path begins at the coordinate pair (i, j) if the conditions $\hat{\pi}(i+1, j) \neq \hat{\pi}(i, j)$, and $\hat{\pi}(i, j-1) \neq \hat{\pi}(i, j)$ are both satisfied, where $\hat{\pi}(i, 0) \equiv 0, \forall i$. A coordinate pair (i, j) that does not satisfy the preceding criteria is a member of a pre-existing path. We shall henceforth let $p(\hat{\pi})$ denote the number of paths possessed by $\hat{\pi}$.

Consider the scalar product

$$(62) \quad S_B(q) := \langle 0 | \prod_{j=1}^{\infty} \hat{\Gamma}_+ \left(q^{\frac{-2j+1}{2}} \right) \prod_{k=1}^{\infty} \hat{\Gamma}_- \left(q^{\frac{2k-1}{2}} \right) | 0 \rangle$$

$$(63) \quad = \sum_{\hat{\mu}} \langle 0 | \prod_{j=1}^{\infty} \hat{\Gamma}_+ \left(q^{\frac{-2j+1}{2}} \right) | \hat{\mu} \rangle \langle \hat{\mu} | \prod_{k=1}^{\infty} \hat{\Gamma}_- \left(q^{\frac{2k-1}{2}} \right) | 0 \rangle$$

where q is an indeterminate and $\sum_{\hat{\mu}}$ denotes a sum over all strict Young diagrams $\hat{\mu}$. We have seen that $\hat{\Gamma}_+(z)|\hat{\mu}\rangle$ and $\langle \hat{\mu}|\hat{\Gamma}_-(z)$ generate all strict Young diagrams $\hat{\nu} \prec \hat{\mu}$, with weightings given by Lemma 2. It follows that equation (63) generates a weighting equal to

$$\prod_{j=1}^M \langle \hat{\nu}_{-j} | \hat{\Gamma}_+ \left(q^{\frac{-2j+1}{2}} \right) | \hat{\nu}_{-j+1} \rangle \prod_{k=1}^N \langle \hat{\nu}_{k-1} | \hat{\Gamma}_- \left(q^{\frac{2k-1}{2}} \right) | \hat{\nu}_k \rangle = 2^{p(\hat{\pi})} \prod_{j=-M}^N q^{|\hat{\nu}_j|}$$

for all diagonally strict plane partitions given by

$$\hat{\pi} = \{\emptyset = \hat{\nu}_{-M} \prec \dots \prec \hat{\nu}_{-1} \prec \hat{\nu}_0 \succ \hat{\nu}_1 \succ \dots \succ \hat{\nu}_N = \emptyset\}$$

Notice that, as explained earlier, due to the powers of 2 appearing in Lemma 2, starting at the main diagonal slice of $\hat{\pi}$ and working outwards, a factor of 2 is acquired for every path in $\hat{\pi}$. This explains the weighting of $2^{p(\hat{\pi})}$ in the above equation. Hence

$$S_B(q) = \sum_{\hat{\pi}} 2^{p(\hat{\pi})} q^{|\hat{\pi}|}$$

Applying the commutation relation (54) successively to equation (62), one recovers a product form for the generating function $S_B(q)$:

$$(64) \quad S_B(q) = \prod_{n=1}^{\infty} \left(\frac{1+q^n}{1-q^n} \right)^n$$

7.2. The neutral fermion two-dimensional Toda lattice hierarchy. The generating function (64) is a specialization of

$$(65) \quad S_B(\mathbf{x}, \mathbf{y}) = \sum_{\widehat{Y}} 2^{-n(\widehat{Y})} Q_{\widehat{Y}}(x_1, x_2, \dots) Q_{\widehat{Y}}(y_1, y_2, \dots) = \prod_{i,j=1}^{\infty} \frac{1+x_i y_j}{1-x_i y_j}$$

where $Q_{\widehat{Y}}$ is the Schur Q -function associated to the strict Young diagram \widehat{Y} [4], and $n(\widehat{Y})$ is the number of non-zero elements in \widehat{Y} , to $\{\mathbf{x}\} = \{\mathbf{y}\} = \{q^{\frac{1}{2}}, q^{\frac{3}{2}}, \dots\}$. We postulate that under a suitable change of variables, S_B is a tau function of the neutral fermion analogue of the Toda hierarchy of the type studied in [11, 12].

ACKNOWLEDGEMENTS

OF wishes to thank Prof T Shiota and Prof K Takasaki for discussions. MW and MZ are supported by Australian Postgraduate Awards.

REFERENCES

- [1] A OKOUNKOV AND N RESHETIKHIN, *Amer. Math. Soc.* **16** (2003) 581–603 [math.CO/0107056](https://arxiv.org/abs/math/00107056)
- [2] T MIWA, M JIMBO AND E DATE, *Solitons: Differential Equations, Symmetries and Infinite Dimensional Algebras*, Cambridge University Press, 2000.
- [3] M JIMBO AND T MIWA, *Publ. RIMS, Kyoto Univ.* **19** (1983) 943–1001
- [4] I G MACDONALD, *Symmetric Functions and Hall polynomials*, Oxford University Press, 1995.
- [5] O FODA AND M WHEELER, *J of High Energy Physics* (2007) no. 1, 075.
- [6] M VULETIĆ, *Int Math Res Notices IMRN* (2007) Article 043.
- [7] M VULETIĆ, *A generalization of MacMahon's formula*, to appear in *Trans. of the American Math Society*, <http://lanl.arxiv.org/abs/0707.0532>.
- [8] K UENO AND K TAKASAKI, *Proceedings of the Japan Academy, Series A, Mathematical Sciences* **59** (1983) 167–170.
- [9] K UENO AND K TAKASAKI, *Advanced Studies in Pure Mathematics* **4** (1984) 1–95.
- [10] K TAKASAKI, *Advanced Studies in Pure Mathematics* **4** (1984) 139–163.
- [11] A YU ORLOV, *Theoretical and Mathematical Physics* **137** (2003) 1573–1588.
- [12] A YU ORLOV AND J C C NIMMO, *Glasgow Math J* **47** (2005) 149–168.

DEPARTMENT OF MATHEMATICS AND STATISTICS, UNIVERSITY OF MELBOURNE, PARKVILLE, VICTORIA 3010, AUSTRALIA.

E-mail address: foda, mwheeler, mzap@ms.unimelb.edu.au